Rev. Adv. Mater. Sci. 33 (2013) 203-210

SURFACE CHARACTERISTICS OF MODIFIED POPLAR WOOD-FLOUR AND ITS EFFECT ON THE MECHANICAL PROPERTIES OF WOOD POLYMER COMPOSITES

Chaoqun Mei[1], Yongming Fan[1], Lei Mei[2] and Guanqun Luo[3]

[1]College of Material Science and Technology, Beijing Forestry University, Beijing 100083, China
[2]College of Chemistry and Molecular Engineering, Peking University, Beijing 100871, China
[3]Department of Forest Products, University of Idaho, Moscow, ID 83844-1132, USA

Received: October 17, 2011

Abstract. In order to characterize properties of wood-flour (WF) and to elucidate their effects on the mechanical properties of wood polymer composites (WPCs), the surface functional groups of modified and unmodified WF were investigated with Fourier transform infrared spectroscopy (FT-IR), the contact angles of different liquids against modified and unmodified poplar WF with 4% maleic anhydride were measured with capillary rise methods based on Washburn equation, the surface free energy and the correspondent dispersive and polar components were calculated through the methodology suggested by Owens-Wendt-Kaelble. The results showed that there was a reduction in the absorbance of hydroxyl groups after the modification; the surface free energy of WF increased from 23.43 mJ/m^2 to 48.31 mJ/m^2, which was higher than the surface free energy (31.2 mJ/m^2) of high-density-polyethylene (HDPE), and its correspondent polar component decreased from 18.79 mJ/m^2 to 0.4 mJ/m^2 and the dispersive component increased from 4.64 mJ/m^2 to 47.91 mJ/m^2 after the modification with 4% maleic anhydride, which made it ready for the spreading of HDPE on the surface of WF. The tensile strength and flexural strength of the WPC samples produced with the modified WF were obviously improved due to the modification. The improved compatibility between WF and HDPE was well confirmed by scanning electron microscopy (SEM).

1. INTRODUCTION

In the last decades, as a result of growing environmental awareness, an interest in the use of natural materials for different applications increased [1-5]. The use of wood as reinforcing filler in polymer composite has shown advantages such as high-specific strength, low cost, low-density, biodegradability, low water absorption and thickness swelling [6-9]. It has also been demonstrated that wood polymer composites (WPCs) exhibit higher resistance to checking, decay, termites, and marine organisms compared to wood [10].

However, despite the attractive properties, the use of WPCs in structural applications is still limited by the lack of performance under specific loading which can be ascribed to the poor adhesion between wood and thermoplastic. Hence, most researchers have focused on surface treatment to the wood (delignification, acetylation, alkaline treatment, and chemical grafting) and using various coupling agents to improve the wood and polymer interface. Chemical coupling agents usually act as bridge to link polar wood fiber and non-polar thermoplastics. This helps transfer the stresses between fibers and polymeric matrices, thus improving the interfacial bonding

Corresponding author: Yongming Fan, e-mail: fanym@bjfu.edu.cn

strength in wood-polymer composites. In some cases it is verified that the use of coupling agents also served to moderate and mitigate moisture movement in the composite, thus improving the mechanical properties of the materials [11-12]. There are many reports related to wood modification using chemical coupling agents. Cui *et al*. [13] used maleated polypropylene (MAPP), together with three surface treatments (an alkaline method, a silane method and an alkaline followed by silane method) to improve the interfacial adhesion between wood and high-density-polyethylene (HDPE) and evaluated the surface chemistry of the treated fibers using FTIR techniques. Zhang *et al*. [14] synthesized poly (N-acryloyl dopamine) (PAD) through free-radical homopolymerization of N-acryloyl-O, O2-diphenylmethyldopimine and subsequent deprotection and studied the adhesive ability to wood. Nourbakhsh *et al*. [15] studied the effect of adding a novel coupling agent, polybutadiene isocyanate, on the mechanical properties of hardwood aspen fiber/polypropylene (PP) composites. Geng *et al.* [16] investigated a novel wood-plastic compatibilizer system containing a paper wet-strength agent (Kymene, a polyaminoamide-epichlorohydrin adduct) as a wood-binding domain and stearic anhydride as a polyethylene (PE) binding domain. Kuang *et al*. [17] used two novel coupling agents for manufacturing wheat straw (WS)/recycled low density polyethylene (LDPE) composites, one being waterborne polyacrylate latex (PAL), the other being blend prepared from polymethylene polyphenylene isocyanate (PAPI) and the PAL. In these studies, the author evaluated the surface characteristics of the modified wood fibers by FTIR techniques or investigated the effect of coupling agents by testing the mechanical properties of WPCs. There are not many reports related to evaluate the characteristics of wood fibers by a quantitative method.

In this study, an attempt was to evaluate the characteristics of treated and untreated wood fibers by surface free energy and its components. Maleic anhydride was used as the coupling agent and the contact angles of different liquids against poplar WF were measured with capillary rise methods based on Washburn equation, then the surface free energy and the correspondent dispersive and polar components were calculated through the methodology suggested by Owens-Wendt-Kaelble. The effect of surface characteristics of wood fibers on the mechanical properties of wood-plastic composites was also investigated.

2. EXPERIMENTAL

2.1. Materials

High-density-polyethylene (HDPE) was obtained from PetroChina Company Ltd. under the trade name T60-800 with a density of 0.963 g/cm^3, and a melt index 6-8 g/10min at 190 °C.

The poplar wood fibers used in this study were collected from a local sawmill and subsequently, were manually screened on a sieve and 40-60 mesh particles were collected, and then were dried in an oven at 105 °C for 24 h to a moisture content ~3%.

Maleic anhydride, methanol, formamide were provided by Beijing Chemical Plant, and distilled water was prepared in the laboratory by ourselves.

2.2. Surface treatment of wood-flour and analysis

2.2.1. Surface treatment

The poplar wood fibers were esterified using 4% maleic anhydride in an SHR-50A high-speed mixer at 120 °C for 5 min and stored in a sealed bag for evaluating the characteristics and preparing samples.

2.2.2. FTIR spectroscopy

FTIR spectroscopy was conducted on a Tensor 27 spectrophotometer (Bruker Optik GmbH) to provide a detailed analysis of the functional groups presented on the surface of untreated and treated WF. Scans were run at a resolution of 4 cm^{-1}. Each WF sample record consisted of 32 scans recorded in absorbance units from 4000 to 650 cm^{-1}. The spectra were obtained with attenuated total reflectance (ATR). The surfaces of WF samples were contact with a ZnSe crystal that had a 45° angle of incidence.

2.2.3. Contact angle measurements

According to Washburn equation [18,19]:

$$h^2 = \frac{\gamma_L R t \cos\theta}{2\eta}, \quad (1)$$

where h is the height of liquid penetration into the capillary at time t; γ_L is the surface free energy of liquid; η is the viscosity of liquid; θ is the contact angle of the liquid against a solid; R is the average effective radius of capillary.

If make

$$K = \frac{\gamma_L R \cos\theta}{2\eta}. \quad (2)$$

Eq. (1) will be transformed into

$$h^2 = Kt. \quad (3)$$

K can be obtained from the coefficient of the equation of h^2-t based on the experiment.

Then

$$R = \frac{2K\eta}{\gamma_L \cos\theta} \quad (4)$$

and

$$\cos\theta = \frac{2K\eta}{\gamma_L R}. \quad (5)$$

The contact angles of different liquids against a solid can be determined by the equation of h^2-t. The WF system can be considered as a capillary system, and the average effective radius of capillary can be considered as a constant when the filled conditions (the filled speed, height and weight) of WF in the glass tube are identical, it can be calculated as per the liquid whose contact angle against WF is zero. Then the contact angles of other liquids against WF can be obtained according to Eq. (5).

The poplar WF was filled in the glass tube under the same condition (the same speed, height and weight), and then the filled glass tubes were fixed upon the liquid for 2 h to reach adsorption balance of liquid molecules on the surface of WF. After that, the height of glass tube was adjusted to make sure the glass tube was in the liquid for 2 mm. When the liquid rose to the 2 mm scale line, the stopwatch began to work, and the height (h) of liquid in the glass tube and the time (t) of rising were recorded at a certain interval. Six replicates were tested for a certain liquid and the mean was used.

2.2.4. Calculation of surface free energy and its polar component

The principle of calculating the surface free energy of a solid and its polar component through the contact angles of liquids against the solid is the equation of Young [20-22]:

$$\gamma_{SV} = \gamma_{SL} + \gamma_{LV} \cos\theta, \quad (6)$$

where γ_{SV} is the surface free energy of a solid which is equilibrated with the steam of liquid; γ_{SL} is the free energy of liquid-solid interface; γ_{LV} is the surface free energy of a liquid; θ is the contact angle of a liquid against the solid.

According to the viewpoint of Owens-Wendt-Kaelble [23,24], the surface free energy of a solid can be divided into dispersive and polar components and the summation of the components is approximately equal to the surface free energy of the solid ($\gamma_S^0 = \gamma_S^d + \gamma_S^p$). If there exist interactions of dispersion and polar forces between a solid and a liquid, the free energy of the interface between the liquid and the solid can be determined by the following equation:

$$\gamma_{SL} = \gamma_{LV} + \gamma_S^0 - 2\left(\gamma_S^d \times \gamma_{LV}^d\right)^{1/2} - 2\left(\gamma_S^p \times \gamma_{LV}^p\right)^{1/2}, \quad (7)$$

where γ_{SL} is the free energy of the interface between a liquid and a solid; γ_{LV} is the surface free energy of the liquid; γ_S^0 is the surface free energy of the solid; γ_S^d is the dispersive component of the surface free energy of the solid; γ_S^p is the polar component of the surface free energy of the solid; γ_{LV}^d is the dispersive component of the surface free energy of the liquid; γ_{LV}^p is the polar component of the surface free energy of the liquid.

Then combine Eq. (7) with Eq. (6) and the difference between γ_S^p and γ_{LV} was ignored [24], the following equation can be obtained:

$$\gamma_{LV}\left(1+\cos\theta\right) = 2\left(\gamma_S^d \times \gamma_{LV}^d\right)^{1/2} + 2\left(\gamma_S^p \times \gamma_{LV}^p\right)^{1/2}. \quad (8)$$

In Eq. (8), only γ_S^d and γ_S^p are unknown. if we can find two liquids whose γ_{LV}^d and γ_{LV}^p are known, γ_S^d and γ_S^p can be calculated through the contact angles of the two liquids against the solid.

Here methanol was chosen as the liquid whose contact angle against the poplar WF is zero because of its low surface free energy. Therefore, the average effective radius of capillary R can be calculated as per the Eq. (4). Then the contact angles of methanol and formamide against the poplar WF can be obtained from Eq. (5). The γ_S^d and γ_S^p of poplar WF can be calculated by Eq. (8).

The dispersive and polar components of the surface free energies and viscosities of the liquids in the experiment were given in Table 1.

2.3. Compounding and sample preparation

The untreated and treated poplar wood fibers were compounded with HDPE at the ratio 60:40 (wt/wt) in the SHR-50A high-speed mixer at room temperature, respectively. The mixture was processed with a Giant SHJ-30 twin-screw extruder

Table1. The surface free energies, corresponding components [25] and viscosities of probe liquids.

Liquids	Items				
	γ_{LV} [mJ/m^2]	γ^d_{LV} [mJ/m^2]	γ^p_{LV} [mJ/m^2]	η* [mN·s/m^2]	η** [mN·s/m^2]
Distilled water	72.8	21.8	51	1.272	1.181
Formamide	57.9	34.4	23.5	4.934	4.222
Methanol	22.5	22.5	0	0.688	0.664

η* and η** were the viscosities of the liquids at the ambient temperature which were measured by Ubbelohde viscometer, respectively.

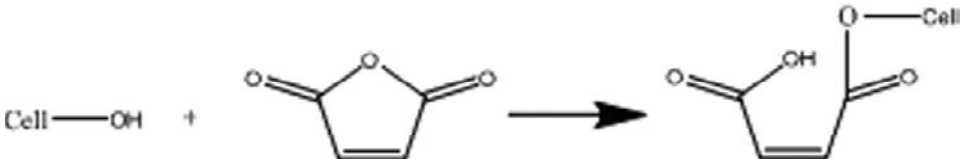

Fig. 1. Mechanism of esterification of wood fibers.

to make composite pellets. The temperatures of the first to the last chambers were 130, 135, 140, 140, 130 °C, respectively. The rotational speed was 20 rpm. Then the composite pellets were extruded in an XSS-300 single-screw extruder with a die. The temperatures of the first to the last chambers were 150, 160, 165 °C and the die was 150 °C. The screw rotational rate was 15 rpm.

2.4. Mechanical properties test

The mechanical behavior of the composites was characterized via tensile and flexural tests in accordance with ASTM Standards D 638 and D 790, respectively. Strength measurements of samples were conducted using an Instron testing machine (Model 1186). The crosshead speed of tension testing was 10 mm/min. Six specimens were tested in each experiment to obtain a reliable average value. Prior to testing, all specimens were conditioned at 23±2 °C, 50±5% RH for at least 40 h according to ASTM D 618.

2.5. Scanning electron microscope (SEM) characterization of fracture surface

Morphologies were observed with a HITACHI S-3000N SEM to examine the fractured surface of the composite samples. Prior to observation, the fractured surfaces of the specimens were coated with a thin gold layer by using a sputter coater.

3. RESULTS AND DISCUSSION

3.1. FTIR spectroscopy

Fig. 1 shows the mechanism of esterification of wood fibers. Fig. 2 shows the characteristic spectra of untreated and treated wood fibers. As can be seen, the broad peak at 3344 cm^{-1} in both spectra is associated with the remaining OH groups of the fiber constituents. There is a reduction in absorbance in this band for the treated wood fibers which implies that there are fewer OH groups remaining. The peak at 2923 cm^{-1} is due to CH asymmetrical stretching vibration in —CH_2— groups and the peak at 2852 cm^{-1} corresponds to CH symmetrical stretching vibration. The peak at 1028 cm^{-1} is assigned to a

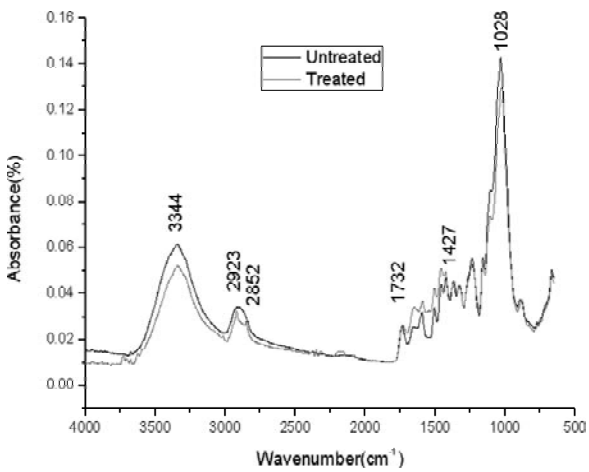

Fig. 2. FTIR spectra of untreated and treated wood fibers.

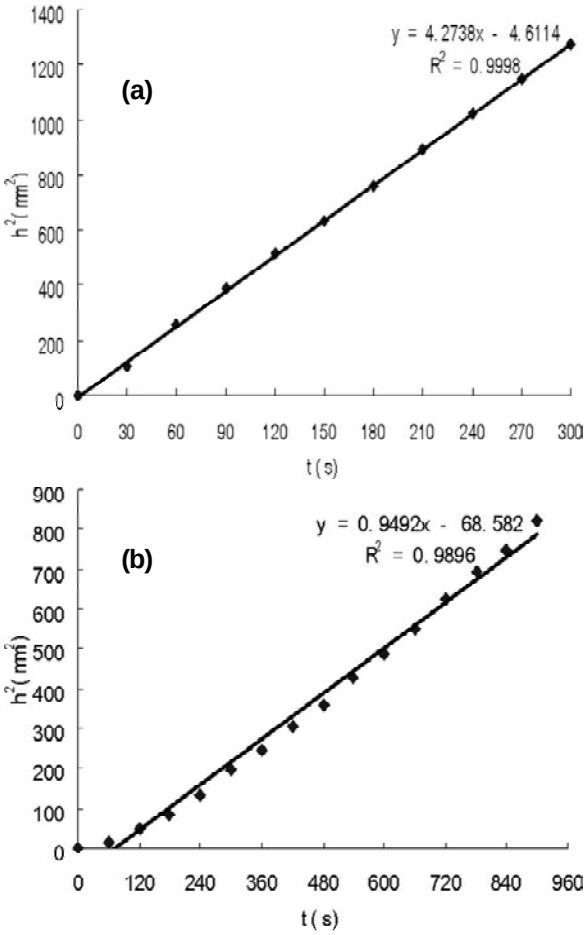

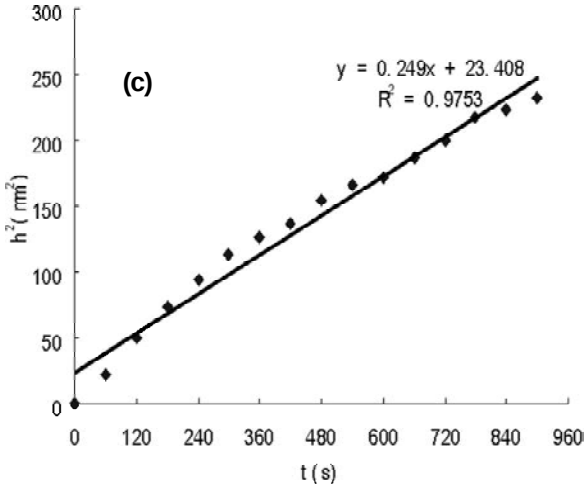

Fig. 3. The curves of h^2-t of three liquids against the untreated WF. (a) The curve of h^2-t of methanol against the untreated WF; (b) The curve of h^2-t of distilled water against the untreated WF; (c) The curve of h^2-t of formamide against the untreated WF.

hydroxyl group associated with cellulose [26] and there is also a reduction in absorbance in this band for the treated wood fibers.

3.2. The contact angles of three liquids against the untreated and treated WF

Fig. 3 and Fig. 4 show the curves of h^2-t of three liquids against the untreated and treated WF. The values of K and cosine of contact angles of the liquids against the untreated and treated WF were listed in Table 2.

3.3. The surface free energies and its components of the untreated and treated WF

The surface free energies and its components of the untreated and treated WF were derived from putting the values of cosθ, γ_{LV}^{d}, and γ_{LV}^{p} of distilled water and formamide in the equation (8) and were listed in Table 3. From Table 3, we can see that the surface free energy of the raw poplar WF is 23.43 mJ/m² and the corresponding dispersive and polar components are 4.64 mJ/m² and 18.79 mJ/m², respectively. After esterified using 4% maleic anhydride, the surface free energy of the treated

Table 2. The values of K and cosine of contact angles of three liquids against the untreated and treated WF.

Liquids	Types			
	Untreated WF		Treated WF	
	K	cosθ	K	cosθ
Methanol	4.2738	1.0000	3.6475	1.0000
Distilled water	0.9492	0.1269	0.0774	0.01167
Formamide	0.2490	0.1623	0.7499	0.50796

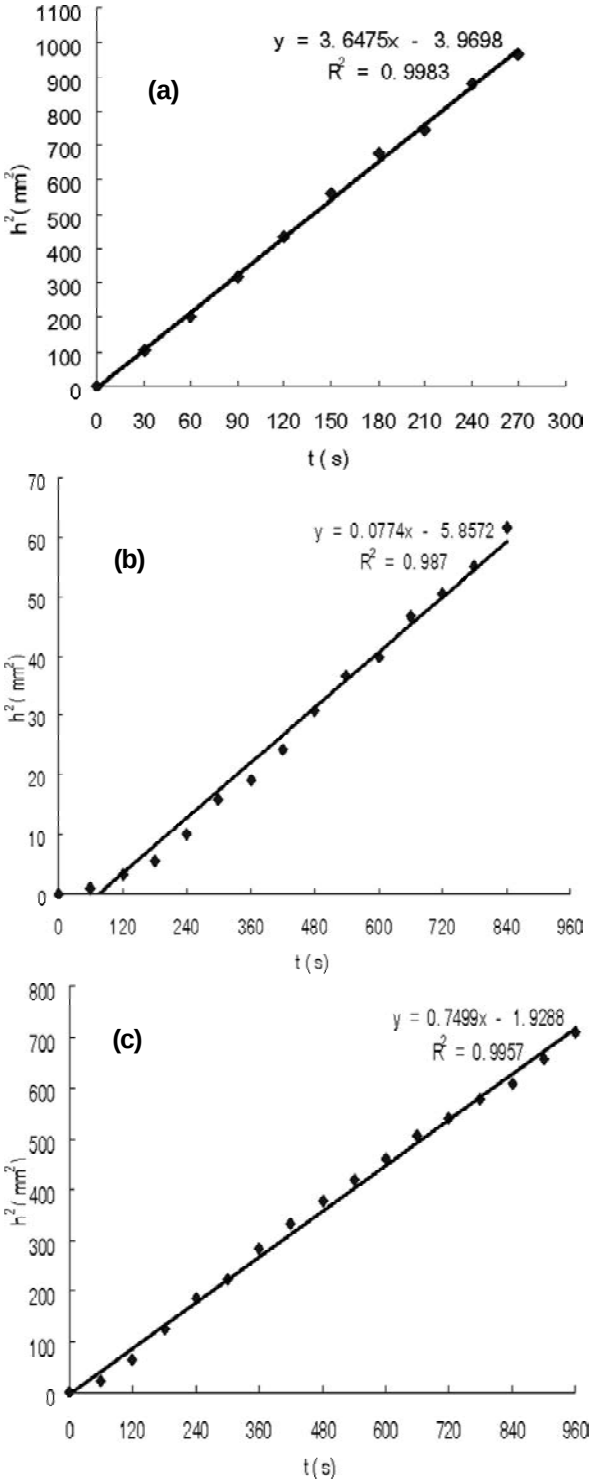

Fig. 4. The curves of h^2-t of three liquids against the treated WF. (a) The curve of h^2-t of methanol against the treated WF; (b) The curve of h^2-t of distilled water against the treated WF; (c) The curve of h^2-t of formamide against the treated WF.

poplar WF is 48.31 mJ/m^2 and the corresponding dispersive and polar components are 47.91 mJ/m^2 and 0.4 mJ/m^2, respectively. According to the standpoint of Zisman [27-30], only when the surface tension of a liquid is less than the critical surface tension (γ_c) of a solid, the liquid can spread on the solid surface. HDPE is in liquid form at the processing temperature and its surface free energy is 31.2 mJ/m^2 [31], it is below the surface free energy of the treated poplar WF, so HDPE can spread on the surface of the treated poplar WF and it is possible for forming a good interfacial adhesion between HDPE and the treated poplar WF.

3.4. Mechanical properties

The tensile strength and flexural strength of WPCs with untreated and treated poplar WF are shown in Fig. 5. The tensile strength of the composites with the poplar WF treated by 4% maleic anhydride increased by about 50% and the flexural strength increased by about 40%. Maleic anhydride has a positive on the mechanical properties of the composites, because it strengths the interfacial bonding between the wood fiber and the matrix polymer, which resulted in good stress propagation and improved the mechanical performance.

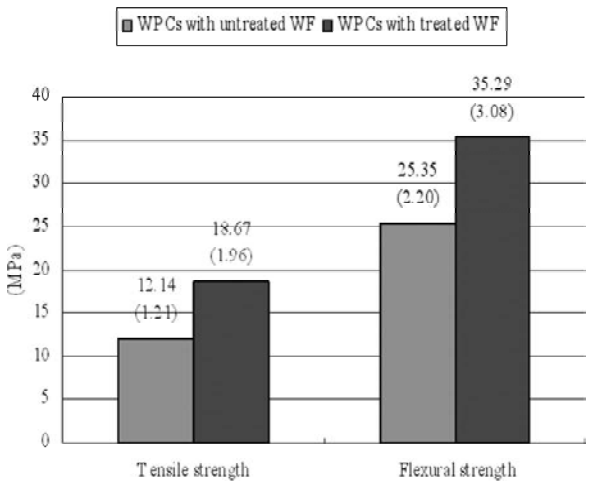

Fig. 5. Tensile strength and flexural strength of WPCs with untreated and treated WF (values in parentheses are standard deviations).

Table 3. The surface free energies and its components of the untreated and treated. WF

Types	Items		
	γ_S [mJ/m^2]	γ_S^d [mJ/m^2]	γ_S^p [mJ/m^2]
Untreated WF	23.43	4.64	18.79
Treated WF	48.31	47.91	0.4

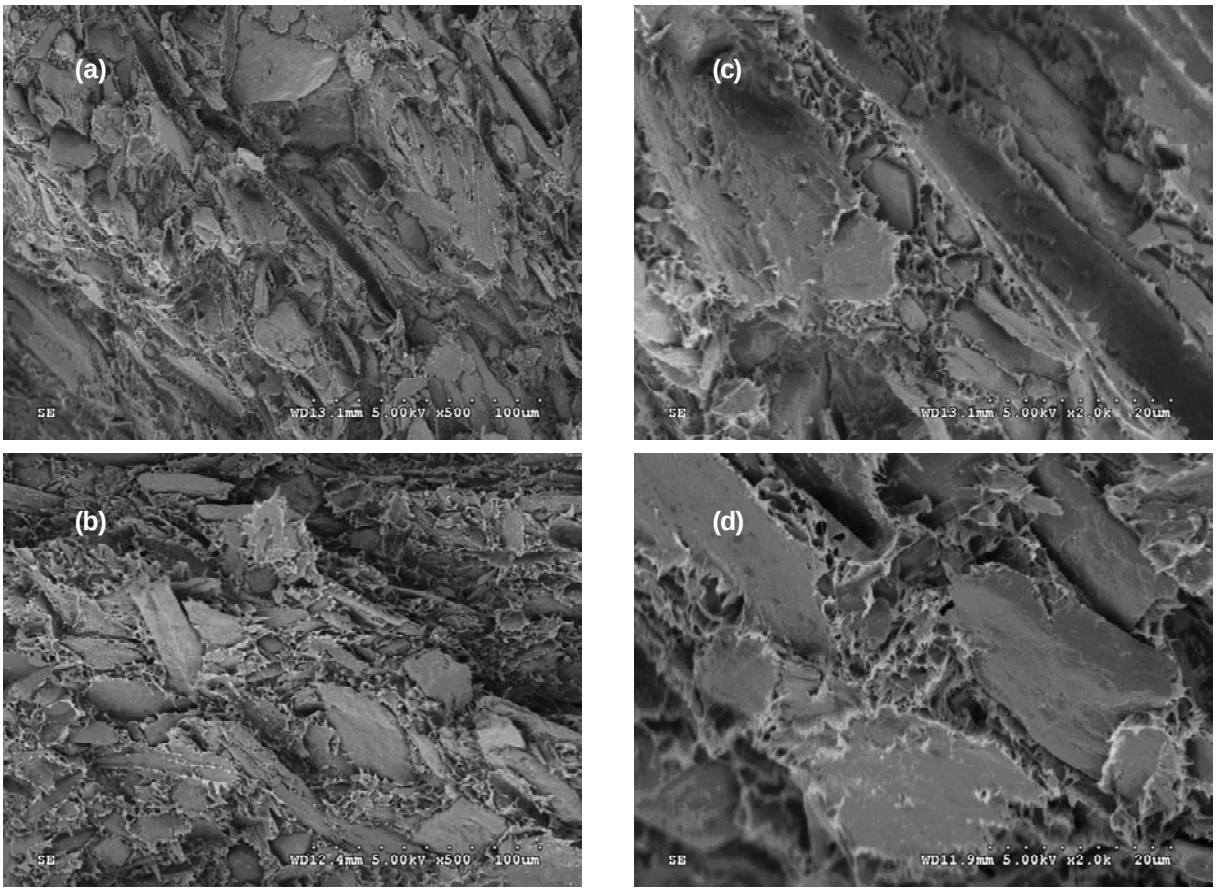

Fig. 6. Flexural fracture surfaces of WPCs with untreated and treated WF. (a) Untreated; (b) Untreated; (c) Treated; (d) Treated.

3.5. Morphological study

As reported in the literature, the morphology of polymer composites is a very important characteristic because it determines the physico-mechanical properties [32]. In this study, the state of the matrix/filler interface of with and without maleic anhydride as coupling agent was investigated by SEM.

Fig. 6 shows the SEM micrographs of the fracture surfaces of WPC samples with untreated and treated poplar WF. As shown in Figs. 6a and 6b, the surfaces of the wood fibers are quite smooth and cavities can be seen between WF and the matrix polymer, these clearly indicate the poor interfacial adhesion between WF and the matrix polymer. This result contributes to the poor stress transfer from matrix polymer to WF leading to poor mechanical properties. Fig. 6c and d shows the SEM micrographs taken from the fracture surface of the WPC samples with treated poplar WF. It can be observed better polymer/filler interfacial adhesion than in the WPC samples with untreated poplar WF resulting in a reduction of the interfacial tension between WF and the matrix polymer. This would be expected to increase the mechanical properties of the composites. This conclusion can be supported by the tensile strength and flexural strength values of WPCs shown in Fig. 5.

4. CONCLUSIONS

The study shows that the surface free energy of the raw poplar WF is 23.43 mJ/m^2 and its correspondent dispersive and polar components are 4.64 mJ/m^2 and 18.79 mJ/m^2, respectively. After the modification with 4% maleic anhydride, there was a reduction in absorbance of hydroxyl groups, the surface free energy increased to 48.31 mJ/m^2 which was higher than the surface free energy of HDPE (31.2 mJ/m^2), and its correspondent dispersive component increased to 47.91 mJ/m^2 and the polar component decreased to 0.4 mJ/m^2. So it was possible for the spreading of HDPE on the surface of the treated poplar WF and forming a good interfacial adhesion between the treated poplar WF and the matrix polymer. This was supported by the mechanical properties and the SEM micrographs of the flexural fracture surfaces of WPC samples.

ACKNOWLEDGEMENTS

The authors would like to acknowledge the financial support of No.2006-55/No.B08005 provided by the National Forestry Bureau and the Ministry of Education of the People's Republic of China.

REFERENCES

[1] J. Simonsen // *Constr. Build. Mater.* **10** (1996) 435.
[2] M.A. Ali, M.A. Khan, K.M.I. Ali, F. Khan and S.R. Ahmad // *Polym.-Plast. Technol. Eng.* **38** (1999) 739.
[3] Y.L. Joo and M.H. Cho // *Int. Polym. Process*. **14** (1999) 10.
[4] P. Hajji, F. Marchand and R. Pirri // *Plast. Rubber Compos*. **37** (2008) 388.
[5] M.C.N. Yemele, A. Koubaa, A. Cloutier and P. Soulounganga // *Wolcott, M. Compos. Pt. A-Appl. S.* **41** (2010) 131.
[6] R. Bouza, A. Lasagabaster, M.J. Abad and L. Barral // *J. Appl. Polym. Sci.* **109** (2008) 1197.
[7] M.A. Khan, K.M.I. Ali and S. Rahman // *Polym.-Plast. Technol. Eng.* **36** (1997) 179.
[8] J. Simonsen, C.M. Freitag, A. Silva and J.J. Morrell // *Holzforschung* **58** (2004) 205.
[9] K.B. Adhikary, S.S. Pang and M.P. Staiger // *Compos. Pt. B-Eng.* **39** (2008) 807.
[10] L. Jiang, M.P. Wolcott, J.W. Zhang and K. Englund // *Polym. Eng. Sci.* **47** (2007) 281.
[11] S.M.B. Nachtigall, G.S. Cerveira and S.M.L. Rosa // *Polym. Test.* **26** (2007) 619.
[12] M. Bengtsson and K. Oksman // *Compos. Sci. Technol.* **66** (2006) 2177.
[13] Y. Cui, S. Lee, B. Noruziaan, M. Cheung and J. Tao // *Compos. Pt. A-Appl. S.* **39** (2008) 655.
[14] C. Zhang, K. Li and J. Simonsen // *J. Appl. Polym. Sci.* **89** (2003) 1078.
[15] A. Nourbakhsh, B.V. Kokta and A. Ashori and A. Jahan-Latibari // *J. Reinf. Plast. Compos.* **27** (2008) 1679.
[16] Y. Geng, K. Li and J. Simonsen // *J. Appl. Polym. Sci.* **91** (2004) 3667.
[17] X. Kuang, R. Kuang, X.D. Zheng and Z.L. Wang // *Carbohyd. Polym.* **80** (2010) 927.
[18] E. W. Washburn // *Phys. Rev.* **17** (1921) 273.
[19] J.T. Davies and E.K. Rideal, *Interfacial Phenomena* (Academic Press, New York and London, 1963).
[20] H.Y. Erbil and R.A. Meric // *Colloid. Surface* **33** (1988) 85.
[21] B. Janczuk and T. Bialopiotrowicz // *J. Colloid Interf. Sci.* **127** (1989) 189.
[22] B. Janczuk and T. Bialopiotrowicz // *J. Colloid Interf. Sci.* **140** (1990) 362.
[23] D.K. Owens and R.C. Wendt // *J. Appl. Polym. Sci.* **13** (1969) 1741.
[24] D.H. Kaelble // *J. Adhes*. **2** (1970) 66.
[25] D.R. Lide, *CRC Handbook of chemistry and physics, Internet version* (Taylor and Francis, Boca Raton, FL, 2007).
[26] N.M. Stark, L.M. Matuana and C.M. Clemons // *J. Appl. Polym. Sci*. **93** (2004) 1021.
[27] H.W. Fox and W.A. Zisman // *J. Colloid Sci.* **5** (1950) 514.
[28] H.W. Fox and W.A. Zisman // *J. Colloid Sci.* **7** (1952) 109.
[29] H.W. Fox and W.A. Zisman // *J. Colloid Sci.* **7** (1952) 428.
[30] A.H. Ellison, H.W. Fox and W.A. Zisman // *J. Phys. Chem.* **57** (1953) 622.
[31] C. Arpagaus, A. Rossi and Rudolf von Rohr // *P. Appl. Surf. Sci.* **252** (2005) 1581.
[32] M. Kaci, S. Cimmino, C. Silvestre, D. Duraccio, A. Benhamida and L. Zaidi // *Macromol. Mater. Eng.* **291** (2006) 869.